ELSEVIER

Biochimica et Biophysica Acta 1326 (1997) 275–286

BIOCHIMICA ET BIOPHYSICA ACTA
BBA

A predicted β-sheet from class S components of staphylococcal γ-hemolysin is essential for the secondary interaction of the class F component

O. Meunier [a], M. Ferreras [b], G. Supersac [a], F. Hoeper [b], L. Baba-Moussa [a], H. Monteil [a], D.A. Colin [a], G. Menestrina [b], G. Prévost [a,*]

[a] *Institut de Bactériologie de la Faculté de Médecine de Strasbourg, 3, rue Koeberlé, F-67000 Strasbourg, France*
[b] *CNR-Cefsa, 14, via Sommarive, I 38050 Povo, Italy*

Received 17 December 1996; revised 6 February 1997; accepted 7 February 1997

Abstract

Site-directed mutagenesis was performed on genes encoding HlgA and HlgC, two of the three proteins expressed from the staphylococcal γ-hemolysin locus, which originate two pore-forming toxins (HlgA + HlgB, HlgC + HlgB). As related proteins, HlgA and HlgC were found to bind first to cell membranes. Amino acid substitutions concerned residues that would predictably disrupt a 13 amino acid conserved β-sheet of the Chou and Fasman secondary structure prediction. The mutation of a threonin into an aspartic acid residue from HlgA (T28D) and from HlgC (T30D) that would break this predicted N-terminal structure lowered dramatically the biological activities on purely lipidic vesicles, erythrocytes and polymorphonuclear cells. The change in secondary structure was confirmed by Fourier Transformed Infrared spectroscopy. The binding of mutated and native proteins at the same kind of sites onto polymorphonuclear cells was evidenced with flow cytometry and fluorescein-labelled anti-class S antibodies or wild type HlgA or HlgC. However, the subsequent binding of fluorescein-labelled HlgB to membrane-bound mutated HlgA or HlgC complexes was inhibited. In conclusion, the first binding of class S components is essential for the subsequent binding of class F components, and a predicted β-sheet seems to be at least one of the functional domains involved. © 1997 Elsevier Science B.V.

Keywords: γ-Hemolysin; Synergy; Sequential binding; Predicted β-sheet; FTIR spectroscopy; Mutagenesis

1. Introduction

The locus encoding the γ-hemolysin from *Staphylococcus aureus* Smith 5R, a methicillin-resistant strain RIMD 310925, P83 and ATCC 49775 strains was described as composed of three genes [1–4]. Two of the corresponding proteins, HlgA and HlgC have primary structures related to the recently described LukS-PV (62–65% identity) and are consid-

Abbreviations: PMN, polymorphonuclear cells; SUV, small unilamelar vesicles; RRBC, rabbit red blood cells; ATR-FTIR, attenuated total reflectance–Fourier-transformed infrared spectroscopy

* Corresponding author. Fax: +33 3 88 251113.

PII S0005-2736(97)00031-X

ered as class S proteins [4]. The third protein, HlgB is related to LukF-PV (72% identity) and considered as a class F protein. Similarly to the pair LukS-PV + LukF-PV which forms the Panton-Valentine leucocidin [5], the γ-hemolysins actually comprise two pairs, e.g., HlgA + HlgB, HlgC + HlgB. The locus encoding γ-hemolysin is largely distributed among *S. aureus* strains, whereas that encoding the Panton-Valentine leucocidin is encountered in only 2% of strains mainly associated with furuncles [6,7]. A 25–30% identity score was found between components of class S and class F [1,4] which may account for a similar folding when integrated into membranes.

In this work we demonstrate that the two γ-hemolysins are pore-forming toxins as the Panton-Valentine leucocidin [8]. Logically, one can expect similar biological features for these compounds, e.g., binding, components interaction, oligomerisation, and formation of the pore. It was reported that LukS-PV and HlgA (class S components) bind first to PMN [9,10] and to rabbit red blood cells [11], respectively. However, HlgB (class F component) was reported to bind primarily onto human RBC [11]. Pairs constituting γ-hemolysin are leucotoxic for various mammalian PMN, monocytes and macrophages [3,4], inducing inflammatory response of host defence cells [9,12–14]. However, HlgC + HlgB exhibits a hemolytic activity very much lower than that of HlgA + HlgB on both rabbit and human erythrocytes.

The different membrane ligands of class S components remain unknown, as well as the interaction between class F components and membrane-bound class S components complexes. Furthermore, the stoichiometric arrangement of the two synergistic proteins participating in pore-formation has still to be defined clearly [9]. The synergistic action of two different proteins and the various cell specificities pertaining to the different pairs of proteins make these toxins rather peculiar. Although the toxic process of such molecules may be the result of pore-formation, other interactions with cell signaling proteins cannot be excluded.

In an attempt to study structure–function relationships within these molecules, a single amino acid substitution was designed to disrupt a part of a predicted secondary structure appearing in both HlgA and HlgC and also in LukS-PV [15]. The biological activity of the purified engineered proteins was analysed on human circulating PMN, rabbit erythrocytes, and small unilamellar vesicles.

2. Materials and methods

2.1. Plasmids and mutagenesis

DNA-modifying enzymes were used as recommended by the manufacturers (Gibco-Bethesda Research Laboratories and New England Biolabs. Beverly, MA). The *hlg* locus of *S. aureus* ATCC 49775 (sequence EMBL Library Databank no. X81586) was previously cloned into the pUC 19 plasmid [16].

Briefly, pairs of oligonucleotides: (1) 3 5′-AATAAATCTTTTAAACATAATGCTA-3′ 27, coupled to 353 5′-TCAAATTGAATGTTTTGA*TC*TATAGCTAATCGT-3′ 326 from *hlgA* sequence determining a HlgA T28D mutated protein and (2) 1475 5′-GCTTTTAGCATTCCAAACAAAAA-3′ 1497 coupled to 1841 5′-GAATTGGATATTTTGA*TC*CACGCCCCATTTATTA C-3′ 1807 or 2132 5′-GTTAAATGATCC*T*TTACCACCAAG-3′ 2109 from *hlgC* sequence determining mutated HlgC T30D, and HlgC N129K, respectively, were used for short DNA fragments amplification [17]. Amplifications were performed in 100 μl containing 10 ng of recombinant plasmid and 2 U of *Taq* DNA polymerase (Gibco-BRL). Operating conditions were as follows: one denaturing step of 4 min at 94°C; 20 cycles of 3 steps of 1 min 30 s at 92°C, 1 min 30 s at 48°C, 1 min 30 s at 72°C; an ending step of 3 min at 72°C. The amplified DNA fragments were electrophoresed on 1.5% (w/v) agarose gel and electroeluted in order to be used in a second amplification with the oligonucleotides 1396 5′-AATGTCTTGCTTTTATTTTT-3′ 1377 and 2845 5′-CTGCAGCTTTAAG-CACTAAAG-3′ 2825, thus amplifying whole *hlgA* and *hlgC* genes, respectively. Secondary amplifications were performed as followed: one denaturing step of 4 min at 94°C; 20 cycles of 3 steps of 1 min 30 s at 92°C, 1 min 30 s at 54°C, 4 min 30 s at 72°C, and 5 min at 72°C. The electroeluted amplified DNA fragments were then ligated to the T/A ended plasmid pCR™II (RD Systems Ltd - London), used to transform *Escherichia coli* (*E. coli*) Invα F′ strain [*endA1*, *recA1*, *hsdR17* (r^-k, m^+k), *supE44*, λ-,

thi1, *gyrA*, *relA1*, ϕ 80, *lacZ* ΔM15 Δ(*lacZYA-argF*), *deoR*$^+$, F′], and sequenced [18] in both strands with T7 DNA polymerase (Pharmacia, Uppsala, Sweden). DNA analyses and structure predictions were made by using DNAStar Software (DNAStar Ltd-London).

2.2. Purification of mutated proteins

For each of the mutated genes as well as for the wild-type gene, recombinant InvαF′ *E. coli* strains were grown at 37°C during 18 h in 2-liter Erlenmeyer flasks filled with 1 liter of 2 × TY medium – 100 μg/ml ampicillin. Bacteria were harvested by a 10-min centrifugation at 7000 × *g* and resuspended as 30% (w/vol) in 50 mM NaH_2PO_4, 1 mM EDTA, 0.5 mM DTT (pH 7.0). Bacteria were then ground under a 130 megaPascal pressure in a FrenchPress (SLM Instruments, Urbana, USA) at 4°C. Bacterial debris were removed by a 35-min ultracentrifugation at 55 000 × *g* in a Ti60 rotor (Beckman) at 4°C. Supernatants were dialysed against 50 mM NaH_2PO_4, 1 mM EDTA, 0.5 mM DTT (pH 7.0). The mutated proteins were purified by the same procedure as previously reported for the wild-type HlgA or HlgC [4,19]. They were stored at −80°C at a 1 mg/ml concentration after being analysed by SDS-PAGE [20] on PHAST®-System (Pharmacia).

2.3. Labelling of antibodies and purified HlgB with 5-([4, 6-dichlorotriazin-2-YL] amino)-fluorescein (DTAF)

Affinity-purified rabbit polyclonal anti-S component antibodies and purified HlgB were adjusted to 1 mg/ml in 0.2 M $NaHCO_3$ (pH 9.0) and mixed for 20 min at room temperature with 0.1 volume of 2 M DTAF solubilised in 1 M $NaHCO_3$ (pH 9.0). The coupling reaction [21] was stopped by equilibrating the solution to 50 mM NH_4Cl (pH 8.0) for 2 H at 4°C. Free DTAF was discarded by desalting in a PD10 column (Pharmacia), and proteins were equilibrated in 30 mM Hepes, 0.15 M NaCl (pH 7.5). DTAF coupling was measured by the determination of the concentration of protein as assayed by Bradford coloration compared to the bound fluorescein concentration measured at $OD_{491\ nm}$ ($\epsilon_M = 61\,000\ M^{-1}.cm^{-1}$). HlgB was labelled with DTAF in a 1:1 mol ratio and conserved more than 95% of the biological activity of the wild HlgB when combined with HlgA or HlgC.

2.4. Secondary structure determinations by attenuated total reflectance – Fourier transformed infrared (ATR-FTIR) spectroscopy

ATR-FTIR spectra were recorded on a Bio-Rad FTS 185 FTIR spectrometer equipped with a DTGS detector with CsI window, a KBr beamsplitter and an ATR attachment by Specac. Typically, 32 interferograms were collected, Fourier transformed to a nominal resolution of 0.5 cm^{-1} and averaged. The instrument was constantly purged with dry air. Spectra were corrected by subtracting a background obtained with the ATR crystal and no sample. The absorbance of residual H_2O was subtracted to give an almost flat baseline between 1880 and 1720 cm^{-1}. Before analysis the leukotoxins were extensively dialysed against three changes of 10 mM Hepes (pH 7.0). For the experiment, 28 to 40 μg of HlgA, HlgA T28D, HlgC, and HlgC T30D contained in 40 μl of the given leukotoxin solution were deposited and dried in a thin layer on one side of a 10-reflections Ge crystal (45° cut): the crystal was housed in a liquid cell and flushed with D_2O-saturated nitrogen for 45 min before collecting the reported spectra.

The ATR-FTIR spectra were processed using the Bio-Rad Win-IR software. Spectra were deresolved to 2 cm^{-1} and then the amide I′ band, between 1600 and 1700 cm^{-1}, was curve-fitted with a sum of Lorentzians, using the nonlinear least squares fitting of Levenberg-Marquardt method [22]. No parameter was constrained. The relative contents of secondary structure elements were estimated by dividing the areas of the individual peaks, assigned to particular secondary structures according to Byler and Susi [23], by the area of the whole amide I′ band; the components around 1610 cm^{-1}, resulting from the side chains, were excluded.

2.5. Permeabilisation of lipid vesicles

Small unilamellar vesicles (SUV) were prepared as follows: an equimolar mixture of phosphatidylcholine (PC, Avanti Polar Lipids) and cholesterol (Cho, Fluka) 1:1 at a total lipid concentration of 2 mg/ml was sonicated for 1 h in a solution containing calcein 80 mM (Sigma), whose pH was adjusted at 7.0 with

NaOH. Titanium particles released by the sonotrode during sonication were removed by centrifugation. SUV were washed in a Sephadex-G25 column to remove free calcein, using a buffer containing 30 mM Tris-HCl, 100 mM NaCl, 1 mM EDTA (pH 7.0).

The permeabilising activity of SUV by the toxins was assayed by measuring the extent of calcein release [24]. In a 1-cm plastic cuvette a total volume of 1.2 ml of the above buffer containing a final lipid concentration around 10 μg/ml and the indicated concentrations of the assayed toxins were incubated under continuous stirring. After the addition of the toxin, the fluorescence (F) emitted at 520 nm (excitation at 494 nm), increased as a consequence of the dequenching of the internal dye when diluted in the external medium. Maximum release was determined by addition of 1 ml Triton X-100. The extent of permeabilisation was calculated as:

$$P(\%) = 100 \times (F_{\text{final}} - F_{\text{initial}})/(F_{\text{maximal}} - F_{\text{initial}})$$

where F_{initial} is the value of fluorescence before the addition of the toxin, F_{final} the value reached at equilibrium, and F_{maximal} the value obtained with Triton X-100.

2.6. Determination of the hemolytic activity

Fresh venous blood was collected from rabbit in EDTA 6 mM. Rabbit red blood cells (RRBC) were prepared by washing thrice (10 min centrifugation at $700 \times g$, broom temperature) in a buffer containing 30 mM Tris-HCl, 100 mM NaCl, 1 mM EDTA (pH 7.0). The time course of the RRBC lysis in the presence of the different toxins was followed by measuring the turbidity at 650 nm in the washing buffer at 25°C, using a kinetic 96-well microplate reader (Molecular Devices UVmax), as already described [25]. Each well contained the specified concentrations of the indicated toxins and RRBC at a concentration of 0.13% (v/v), which corresponds to an initial $A_{650\text{nm}}$ of 0.1, in a final volume of 200 μl of the same buffer. When a couple of toxins was assayed, both components were added at the same concentration, and serially two-fold diluted along a line of the microplate. In competition studies of a native with a mutant toxin, the concentration of the wild-type toxins (HlgA + HlgB or HlgC + HlgB) was constant all along the line, while the mutant was serially diluted. The 96 wells were stirred and read every 8 s for 45 min of reaction. The percentage of hemolysis was calculated as:

$$\text{Hemolysis}(\%) = 100 \times (A_{\text{initial}} - A_{\text{final}})/(A_{\text{initial}} - A_{\text{water-lysed}})$$

where A_{initial} is the absorbance before adding the toxin, A_{final} that after the addition of the toxin, and $A_{\text{water-lysed}}$ the absorbance obtained when the RRBC were completely lysed in water. The maximal rate of hemolysis, V_{max}, was the largest slope calculated in the absorbance vs. time curve normalised by dividing by $(A_{\text{initial}} - A_{\text{water-lysed}})$.

For the end-point measurements, the assay was performed differently. In a total volume of 500 μl, RRBC (at the same final concentration as above) were incubated with the toxins for 30 min at 37°C. Intact cells were pelleted ($15\,800 \times g$, 3 min) and the released hemoglobin in the supernatant was read at 415 nm. The hemolytic activity was calculated as:

$$\text{Hemolysis}(\%) = 100 \times (A_{+\text{toxin}} - A_{-\text{toxin}})/(A_{\text{water-lysed}} - A_{-\text{toxin}})$$

where $A_{+\text{toxin}}$ and $A_{-\text{toxin}}$ are the reading with and without toxin, respectively.

2.7. Preparation of leucocytes

Five ml of Plasmion® (Lab. Roger Bellon, France) were added to 14 ml of buffy-coats from healthy donors diluted with 6 ml of 9‰ (w/v) NaCl and left to sediment for 30 min. Supernatant leucocytes suspension were harvested and the residual erythrocytes contaminating were lysed for 10 min by completing to 50 ml with 0.16 M NH_4Cl. After washing, cells were resuspended (5×10^6 cells/ml) in 140 mM NaCl, 5 mM KCl, 10 mM glucose, 0.1 mM ethylene glycol-bis(beta-aminoethyl ether) N, N, N′,N′-tetra-acetic acid, 10 mM Hepes and 3 mM Tris-base (pH 7.3). The latter buffer was also used to wash cells treated with toxins and antibodies as well as for competition assays before flow cytometry analysis.

2.8. Flow cytometry measurements

Before further experiments, rapid leucocytolytic and hemolytic assays were achieved as previously reported [4]. Flow cytometry measurements were

made using a FACSort® cytometer (Becton-Dickinson, Le Pont de Claix, France) equipped with a 15 mW argon laser tuned at 488 nm. Forward (FSC) and side (SSC) light scatter dot plots acquired from 5000 purified white cells (10^6 cells/ml) were usually gated for PMN [10]. The fluorescence light 1 (FL1: λ_{EM} = 530 nm) was used to record the DTAF fluorescence and the fluorescence light 3 (FL3: λ_{EM} = 585 nm) was used to record the fluorescence of ethidium. The fluorescence of ethidium which increases when it is bound to nucleic acids was used as an indicator of the formation of pores through the cell membrane as previously described in the absence of calcium [10]. Data were calculated from quadriplicate assays by Lysis 2 TM software (Becton-Dickinson, France).

2.9. Binding capabilities determination

Two methods were used to determine the binding of both components: (1) the binding of the class S components was measured by the fixation of fluorescent anti-class S components antibodies. The PMN were incubated with increasing amounts of HlgA or HlgC, and after washing, a 15 min subsequent incubation with fluorescent anti-S antibodies (2.5 μg/ml) was performed at room temperature; (2) the class S components capabilities to bind the class F component were estimated by the binding of fluorescent DTAF-HlgB (0.75 nM). The results were calculated as percent of the mean fluorescence obtained from 5000 cells for 3 nM HlgA or HlgC. A concentration of 3 nM in HlgA and HlgC was used in the rest of this study for mutants comparison and competition since this value is close to the concentration where the specific binding is saturated.

3. Results

3.1. Secondary structure predictions

However, class S proteins, on one hand, and class F proteins, on the other hand, harbour from 60 to 98% sequence identity. Moreover, secondary structure predictions [15] revealed significant homologies. As an attempt to verify the significance of these observations and determine which of the predicted

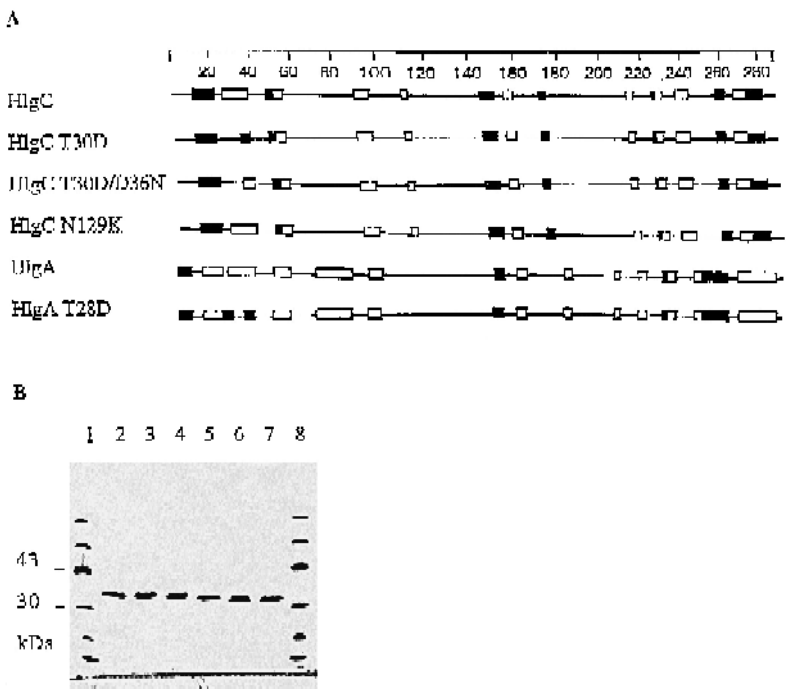

Fig. 1. A: Secondary structures predictions of HlgC, HlgC T30D, HlgC T30D/D36N, HlgC N129K, HlgA, and HlgA T28D. Alpha-helices (□) and beta-sheet (■) predictions were obtained by computed Chou and Fasman [3] algorithms (DNAStar Ltd). B: SDS-PAGE of the purified mutated proteins (50 ng loaded). Lanes 1 and 8: apparent molecular mass ladder (Pharmacia). Lane 2: HlgC. Lane 3: HlgC T30D. Lane 4: HlgC T30D/D36N. Lane 5: HlgC N129K. Lane 6: HlgA. Lane 7: HlgA T28D.

secondary structures may have an important role in the cascade of events determining pore-formation, we introduced amino acid substitutions that would, predictably, disrupt some conserved secondary structures of the class S proteins. These latter components were considered as the most critical to study, since they are binding to target cell membranes in first place.

Two mutations concerned a predicted and conserved 13 amino acid-long β-sheet (Fig. 1A) in the N-terminal extremity of HlgA and HlgC (HlgA T28D and HlgC T30D). A third one HlgC T30D/D36N was obtained simultaneously to HlgC T30D and was analysed because of a predicted partial restoration of the β-sheet along 6 amino acids. The HlgC N129K was induced in order to modify a region (GYNIGG-GNFQS) having homology with some human integrins [26]. The considered secondary structures were predicted by the methods of Chou and Fasman [27] and Garnier et al. [28]. The purified proteins showed comparable molecular mass with the staphylococcal native proteins (Fig. 1B). The biological specific activities of the native staphylococcal proteins were previously observed to be comparable to the *E. coli* recombinant proteins, thus allowing the use of the former proteins in the following experiments.

ATR-FTIR spectra of HlgA and HlgC are shown in Fig. 2. In all cases the amide I′ band is peaked in the region at 1634–1641 cm^{-1}, indicating a prevalence of β structure, at least in part composed of antiparallel β-sheet [23]. Upon introduction of Thr for Asp at position 28 in HlgA and 30 in HlgC there is a reduction in the absorption at 1635 cm^{-1} indicative of a decrease in β-sheet (Table 1). In the case of HlgA T28D such a decrease is compensated mainly by an increase in β-turn structure, whereas in the case of HlgC T30D there is an increase in the unordered structure.

3.2. Permeabilising activity on model membranes

The pairs constituting γ-hemolysins HlgA + HlgB and HlgC + HlgB were both found to have a permeabilising activity on small unilamelar vesicles (SUV).

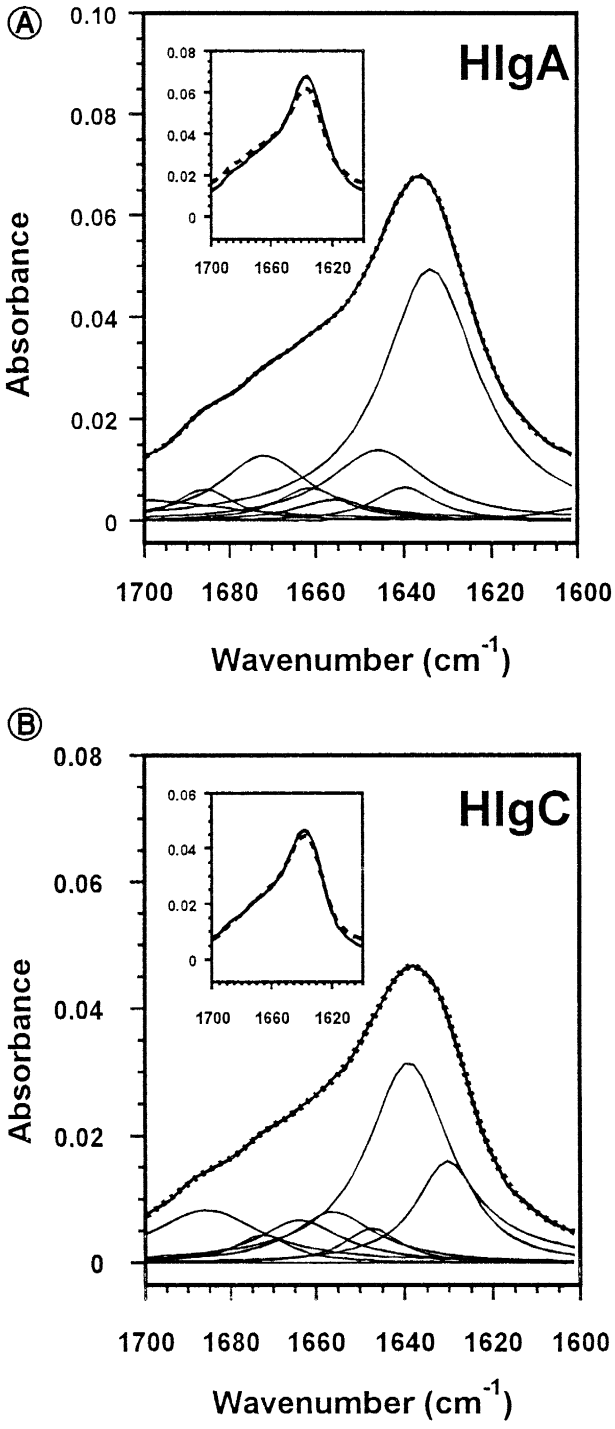

Fig. 2. Infrared-ATR spectra in the amide I′ region of deuterated films of class S components of gamma-lysins. A: HlgA; B: HlgC. The spectrum (solid line), seven Lorentzian component bands obtained by curve-fitting (thin solid lines) and their sum (dotted line), are shown in each case. A linear baseline was subtracted. In the insets, the spectra of the point mutants described in this paper (dashed lines) are compared to the respective wild-type (solid lines). In both cases, the spectrum of mutant was normalised to have the same total area as the wild-type.

Table 1
Secondary structure determination of gamma-lysins and mutants by ATR-FTIR

Protein	β_1	t	a	r	β_2	β_{total}
HlgA	6.7	14.6	5.9	15.8	57.0	63.7
HlgAT28D	9.6	25.4	4.5	17.0	43.4	53.0
HlgC	4.3	21.4	11.0	5.1	58.1	62.5
HlgC T30D	4.7	24.4	11.7	14.0	45.2	49.9

Best fitted Lorentzians (see Fig. 2) were assigned to a particular secondary structure according to Byler and Susi [22]: β_1 pertains to antiparallel β-sheet, β_2 to both parallel and antiparallel β-sheet, α is for α-helix, t for β-turn and r for random coil or, more in general, unordered structure. β_{total} is β_1 plus β_2. The errors, as derived from independent fittings, are within $\pm 5\%$.

Hence, the effect of the mutations HlgA T28D and HlgC T30D on this activity was studied. Fig. 3A shows the extent of calcein release measured when 95 nM of HlgA, HlgC, HlgA T28D or HlgC T30D were incubated with PC:Cho 1:1 SUV in the presence of the same amount of HlgB. HlgA had the highest permeabilising activity, while the mutants were completely inactive, even at concentrations up to five times higher than the wild-type protein (data not shown).

The competition between HlgA T28D and HlgC T30D and the respective wild-type proteins in the permeabilisation of lipid vesicles was then studied. Constant concentrations of HlgA + HlgB or HlgC + HlgB were incubated with SUV (PC:Cho 1:1) in the presence of increasing amounts of HlgA T28D and HlgC T30D, respectively. As shown in Fig. 3B, there was a competition between the mutants and natural proteins, which was stronger in the case of HlgA. At the same concentration of HlgA and its mutant, calcein release decreased to around 40% of control, disappearing almost completely when HlgA T28D: HlgA was in a 4:1 ratio. In the case of HlgC, as the concentration of HlgC T30D increased, the release of calcein decreased, being 15% lower when HlgC and the mutant were equimolar, to reach 50% of the original activity when the mutant was four times more concentrated than the wild-type toxin. Due to the high amount of toxins required in these experiments, a complete decrease of the permeabilising activity of HlgC could not be reached.

3.3. Hemolytic activity

The hemolytic activity of HlgA T28D and HlgC T30D, in the presence of HlgB, was assayed on rabbit red blood cells (RRBC) and compared with that of the wild-type toxins. In these assays, the class S components HlgA or HlgC and HlgB were always added in the same concentration, both the extent of the hemolytic activity and the maximal rate of hemolysis, V_{max} were determined (Fig. 4A,B). HlgA + HlgB provoked 80% of hemolysis at a concentration 4

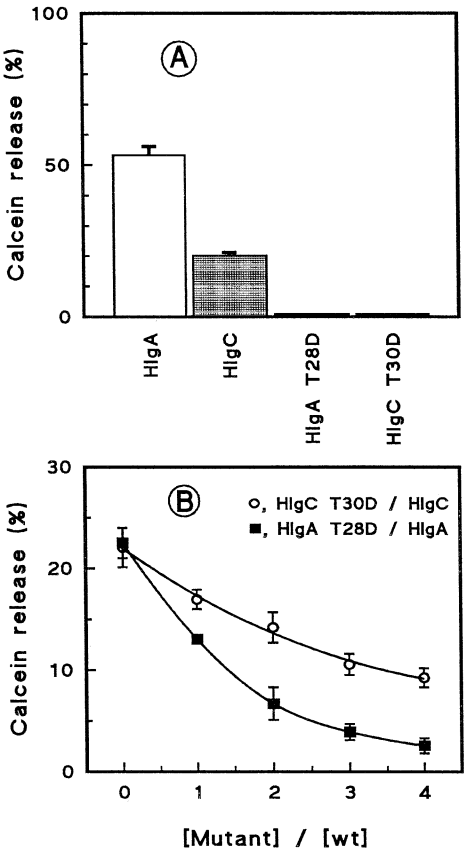

Fig. 3. Permeabilising activity of HlgA, HlgA T28D, HlgC and HlgC T30D, in the presence of equimolar HlgB, on small unilamellar vesicles of PC:Cho 1:1. A: Permeabilising activity, obtained in the presence of 95 nM of each toxin and expressed as the % of calcein released ($n = 2$). Maximal release was the value obtained when vesicles were incubated with Triton X-100. B: direct competitions of the mutants HlgA T28D and HlgC T30D with native HlgA and HlgC, respectively, for SUV permeabilisation. In both cases, a fixed concentration of the native toxins (31.25 nM each for HlgA + HlgB and 95 nM each for HlgC + HlgB) was incubated with increasing concentrations of the mutant ($n = 2$). In this figure, the % of calcein release is represented as a function of the ratio [mutant]/[wild type toxin].

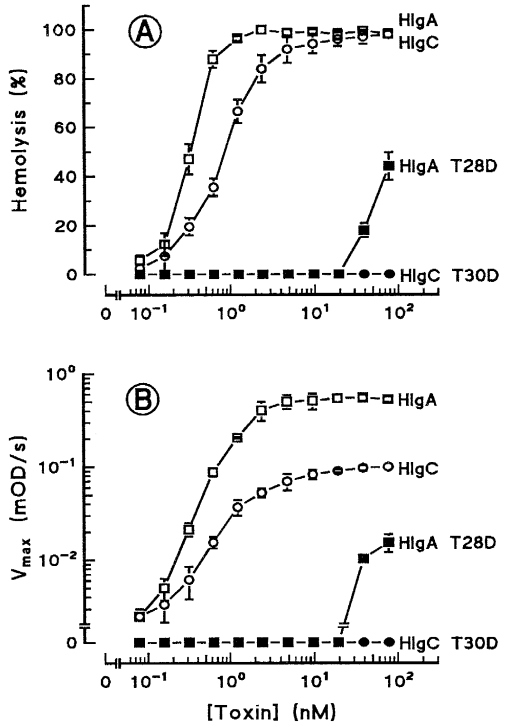

Fig. 4. Titration of the hemolytic activity of HlgA, HlgA T28D, HlgC and HlgC T30D in the presence of HlgB on rabbit red blood cells ($n = 3$). A: extent of hemolysis expressed as a percentage of the maximal hemolysis obtained by incubating the red blood cells with distilled water. B: maximal rate of hemolysis (V_{max}) calculated from the kinetic curves of hemolysis. HlgB was always present at the same concentration than the S component of the couple. The time course of the hemolysis was followed turbidimetrically, and the final % of hemolysis and V_{max} were calculated as described in Section 2.

times lower than HlgC + HlgB (around 0.5 nM and 2 nM, respectively). Titration of V_{max} indicated that, as the concentration of toxins increased over 0.09 nM, V_{max} increased as well, to finally reach a saturating value which was almost ten times higher with HlgA + HlgB than with HlgC + HlgB.

When HlgA T28D was assayed in the presence of HlgB, and compared with HlgA, the mutant presented only a slight hemolytic activity, 250 times lower than that obtained with the wild-type toxin. On the contrary, HlgC T30D was not hemolytic at any of the assayed concentrations, indicating that this mutant is at least 1000 times less active than the native HlgC.

In order to determine whether the mutants HlgA T28D and HlgC T30D were able to bind to the cell membrane, a test of competition was performed between these mutants and the respective native toxins. The assay was performed keeping constant the concentration of the native toxin, while the concentration of the mutant was varied in a range of 5×10^3 times. When RRBC were incubated with HlgC + HlgB and increasing concentrations of HlgC T30D, the hemolytic activity decreased (Fig. 5A), becoming around 70% of the control (native proteins) when HlgC and HlgC T30D were present in equimolar amounts. This indicated the capability of the mutant to bind to the membrane. Similarly, the hemolytic activity of HlgA + HlgB decreased in the presence of increasing amounts of HlgA T28D, being around 70% when HlgA and HlgA T28D were equimolar

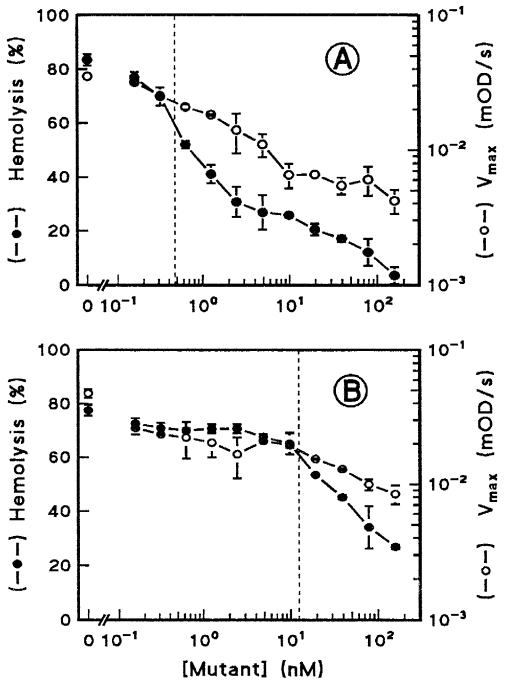

Fig. 5. Hemolytic assays of direct competitions between the native toxins HlgA (A) and HlgC (B) and various concentrations of the mutants HlgA T28D and HlgC T30D (bottom ordinate scale). The mutants were incubated at different concentrations with a fixed concentration of HlgA + HlgB (0.47 nM each) or HlgC + HlgB (12.5 nM each). After the addition of RRBC, the hemolytic activity was measured ($n = 2$) as in Fig. 4. In each panel of this figure, the % of hemolysis (left ordinate scale) and V_{max} (right ordinate scale) are reported as a function of the concentration of the mutant. The dashed line represents the conditions in which native toxin and mutant are present in equimolar amounts.

(Fig. 5B). HlgA T28D at a concentration 300 times higher than HlgA completely removed the hemolytic activity of HlgA.

3.4. Leucotoxic activity

Fig. 6 shows that the pairs HlgA + HlgB and HlgC + HlgB are both able to provoke an influx of ethidium in target cells, indicating the formation of pores through the membrane. HlgA T28D in association with HlgB did not show any ability to form pores through the membrane of PMNs as revealed by ethidium fluorescence (Fig. 6A). Moreover, HlgA T28D was able to inhibit the biological activity of HlgA when it was ten times more concentrated than HlgA. Three HlgC mutants (HlgC T30D, HlgC T30D/D36N, HlgC N129K) were analysed in association with HlgB for their biological activity on PMNs and compared with wild HlgC. HlgC T30D had lost its toxicity towards PMNs (Fig. 6B) as HlgA T28D did. Although HlgC T30D was not toxic, it inhibited the activity of HlgC on human PMNs when it was ten-fold more concentrated (Fig. 6B). The parent mutant HlgC T30D/D36N showed the same lack of biological activity (Fig. 6C), and the same inhibiting properties. Conversely, the mutation in N129 had no significant consequence on the protein activity (data not shown). Thus, HlgC N129K did not receive more attention. At the opposite HlgC T30D, and HlgC T30D/D36N were shown to have lost their toxicity (Fig. 4) as had HlgA T28D.

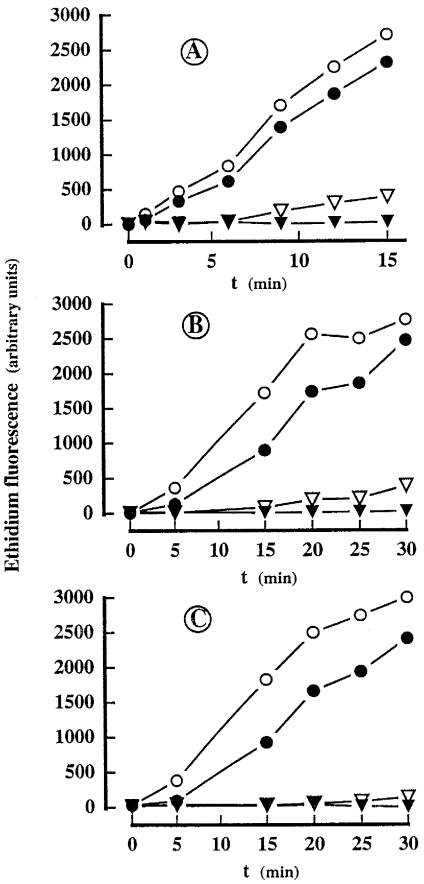

Fig. 6. Determination by flow cytometry of the ethidium fluorescence of PMNs incubated in the presence of A: 0.75 nM HlgB and either 3 nM HlgA (open circles), or 3 nM HlgA + 3 nM HlgA T28D (closed circles), or 3 nM HlgA + 30 nM HlgA T28D (open triangles), or 3 nM HlgA T28D (closed triangles); B: 0.75 nM HlgB and either 3 nM HlgC (open circles), or 3 nM HlgC + 3 nM HlgC T30D (closed circles), or 3 nM HlgC + 30 nM HlgC T30D (open triangles), or 3 nM HlgC T30D (closed triangles); C: 0.75 nM HlgB and either 3 nM HlgC (open circles), or 3nM HlgC T30D + 3nM HlgC T30D (closed circles), or 3 nM HlgC + HlgC T30D/D36N (open triangles), or 3 nM HlgC T30D/D36N (closed triangles).

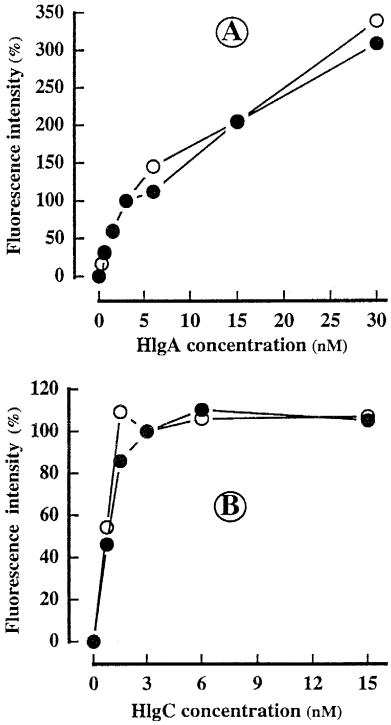

Fig. 7. Flow cytometry analysis of the binding of different HlgA (A) and HlgC (B) concentrations to PMNs revealed by fluorescent antibodies (open circles) and fluorescent HlgB (closed circles). The fluorescence intensity was expressed in % of the value obtained for 3 nM HlgA or HlgC.

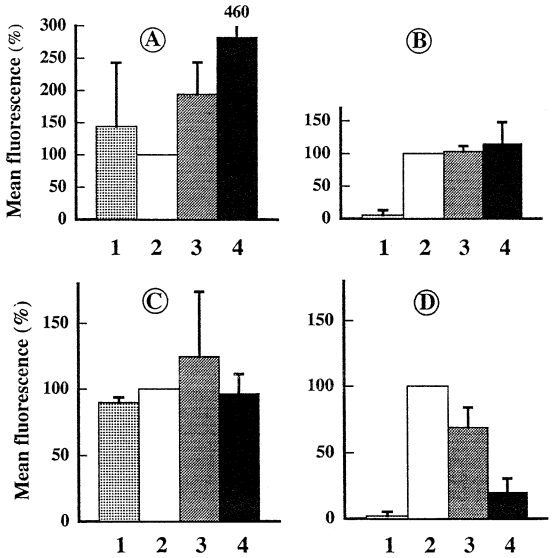

Fig. 8. Determination by flow cytometry of the fluorescence intensity of PMNs measured in the presence of A,C: fluorescent anti S-component antibodies, and B,D: fluorescent DTAB-HlgB. A,B: Mean fluorescence intensities obtained for 3 nM HlgA T28D (1), 3 nM HlgA and 3 nM HlgA T28D (3), 3 nM HlgA and 30 nM HlgA T28D (4) were expressed in % of the value obtained for 3 nM HlgA (2) ($n = 4$). C,D: Mean fluorescence intensities obtained for 3 nM HlgC T30D (1), 3 nM HlgC and 3 nM HlgC T30D (3), 3 nM HlgC and 30 nM HlgC T30D (4) were expressed in % of the value obtained for 3 nM HlgC (2) ($n = 4$).

The use of fluorescent antibodies indicated that the binding of HlgA was composed by a specific and a non-specific part (Fig. 7A), whereas the binding of HlgC seemed strictly specific (Fig. 7B). The properties of these different bindings of HlgA and HlgC will be extensively studied elsewhere. The mutated HlgA retained its ability to bind to PMN membranes, as revealed by the fixation of fluorescent S component antibodies (Fig. 8A). In fact, the amount of fluorescent antibodies bound when HlgA was mixed with HlgA T28D was very similar to that with HlgA alone (Fig. 7A) but at a concentration corresponding to the sum of the concentrations of the two proteins. Interestingly, HlgA T28D lost the capacity to bind HlgB as shown in Fig. 8B using DTAF-HlgB, and this would explain why it had no pore-forming ability. On the contrary, the mutant did not inhibit the binding of HlgB to HlgA since competition experiments did not reveal a decrease in binding. Furthermore, since the results obtained for the binding of DTAF-HlgB were comparable to those for the binding of fluorescent anti S component antibodies, one can conclude that the non-specifically bound HlgA is still functional, at least for the secondary binding of HlgB.

HlgC T30D, like HlgA T28D, retained its ability to bind to human PMN membranes (Fig. 8C) but also competed efficiently with HlgC on its binding site. Finally, membrane-bound HlgC T30D, like HlgA T28D, lost its ability to bind HlgB secondarily (Fig. 8D), and thus, no pores could be formed through the cell membranes. HlgC T30D/D36N behaved exactly as HlgC T30D did (data not shown).

4. Discussion

Staphylococcal leucotoxins appear to be of interest because they operate by the sequential and synergistic action of class S and class F proteins, and they are directed mainly against the host defence cells. Moreover, despite forming a defined toxin family comprising at least 8 characterised and related class S and class F proteins [1–4,29,30], they do not share high sequence identity with other known toxins. For example, staphylococcal α-hemolysin and exfoliative toxins harboured only 29% and 23% identity with class S components, respectively. Exfoliative toxins are rather known as serine-proteases [31]. Homologies between α-hemolysin and leucotoxins may reflect a similar folding of the pores formed by the toxins [32]. However, the sequential binding of proteins constituting leucotoxins remains a fundamental mechanistic process, and oligomerisation might be more easy to study than for α-hemolysin because of the presence of two different proteins.

It has to be emphasized that flow cytometry revealed that pairs constituting the γ-hemolysin are pore-forming toxins as it was demonstrated for the Panton-Valentine leucocidin [10] and that biological activity of these pairs can be studied either with PMN, RRBC and SUV. More details will appear elsewhere concerning the biological properties of γ-hemolysin. Site-directed mutagenesis strategy initially involved a conserved predicted secondary structure within class S proteins bearing membrane affinity. Mutated proteins were purified to homogeneity and it should be noticed that hydrophobic chromatography [4] was necessary to avoid cross-contamination

with HlgB. Here, the biological effect of mutations HlgC T30D, HlgC T30D/D36N and HlgA T28D, that would, predictably, disrupt a conserved 13 amino acid-long β-sheet in the N-terminal part of the class S proteins of gamma-hemolysins (from L25 to K37 for HlgA and from W27 to K39 for HlgC), was reported. Secondary structure evaluations from ATR-FTIR spectra of the mutants and the wild-type toxins were performed, indicating a decrease in β-sheet of around 10% for the mutants, suggesting it involves a total of about 27 residues, therefore, more than the single predicted β-strand containing the mutation. This suggests that the mutated strand may belong to a region of pleated sheets. These mutations were chosen because they represented amino acid substitutions by residues bearing different charge but similar steric space. Another mutation was designed to integrate a positive charge (HlgC N129K) in a short sequence common with human integrins [26] which was not critical for biological activity.

The biological activities of pairs comprising HlgB were dramatically affected for HlgC T30D, HlgC T30D/D36N, and HlgA T28D. The extent of the loss of activity could not always be determined because of the limits in the amounts of proteins available. HlgC T30D did not show any biological activity, neither against natural membranes (PMN and RRBC) nor against model membranes (SUV), so that they are at least 1000 times less active than HlgC. HlgA T28D instead retained some hemolytic activity, albeit 250 times lower than that of the native toxin, but was equally inactive on PMN and on the model of membrane permeabilisation. These observations prompted the analysis of the effective binding of these non-active mutated proteins to the PMN membrane by a three-step procedure. The first step implied native versus mutated proteins competition and the determination of the biological activity by ethidium entry into permeabilised PMN. The results were similar for HlgC and HlgA, and clearly indicated that when equal amounts of wild-type toxins and their respective mutants were applied in addition to HlgB; around 70 to 80% of the activity without the mutants was retained. When mutated proteins were 10-fold more concentrated, the biological activity was almost insignificant as compared to that of natural toxins. The second step was the determination of the binding of mutated proteins by fluorescent antibodies which showed that both the mutated HlgA and HlgC kept their binding properties (specific and non-specific for HlgA, specific for HlgC) and could compete with wild-type proteins on the same binding sites. Therefore, the primary binding of class S components to membranes was once more confirmed. The third one was the determination of the binding of fluorescent HlgB on the bound mutated proteins. They were both shown to be unable to bind HlgB, but, when associated with their respective native protein, they gave different results. HlgA T28D, even ten times more concentrated than HlgA, did not modify the binding of HlgB, suggesting the presence of non-specific binding sites for HlgA for which no significant competition occurred. Nevertheless, there was no opening of pores. An explanation for this could be that the pores, as for α-toxin [33], are constituted by oligomers including several S components where the native toxin and its mutant could be mixed. In these oligomers, HlgB could bind to HlgA but not to the mutated protein, thus rendering the oligomers probably containing both HlgA and the mutated HlgA unable to create a pore. Conversely, in the case of HlgC at the concentration of 3 nM (Fig. 7B), the binding sites are nearly saturated and HlgC T30D can compete with its parent protein, thus decreasing the binding sites of the HlgB class F component. A higher propensity of HlgA to make unspecific binding, presumably to the lipid matrix itself could explain its higher activity on purely lipidic vesicles. Furthermore, the formation of inactive complex aggregates containing native and mutated class S components and class F components is the only reasonable explanation for the competition effect observed with SUV, where specific binding is excluded.

In conclusion, the mutated proteins seemed to bind to the same membrane target sites as the respective native proteins. This indicated that the mutations, although predictably disrupting a 13 amino acid-long β-sheet (from W27 to K39), did not affect profoundly the structural conformation of the whole protein. The loss of pore-forming activity of the mutated toxins was shown to be due to the loss of the ability to make an oligomer with HlgB. At this point of studies, it is not known whether disruption of the β-sheet or the only introduction of a negative charge are responsible for the loss of binding of HlgB. The predicted 13 amino acid long β-sheet appears at least to have an

essential role in the class S component-mediated binding of HlgB (class F component). However, the mutation D36N (HlgC T30D/D36N) did not restore any functional activity although, according to the secondary structure predictions, it retained a putative 6 amino acid-long β-sheet. The latter result would indicate either the secondary structure prediction is fictitious, or that the restored structure is not sufficient to allow the binding of HlgB, or that threonin 30 exerts a critical role in the secondary binding. Contrary to the α-toxin where oligomers can be observed in solution [34], major structural modifications appear to be necessary in order to favour the secondary binding of class F component of leucotoxins. More detailed studies are now in progress together with topology analysis of pore-formation and cristallographic studies.

Acknowledgements

The skillful technical assistance of D. Keller was greatly appreciated. This work was supported in part by grant from the Direction de la Recherche et des Etudes Doctorales (DRED EA 1318). M.F. was supported by a post-doctoral fellowship from the European Community (European Project CHRX-CT93-055).

References

[1] J. Cooney, Z. Kienle, T.J. Foster, P.W. O'Toole, Infect. Immunol. 61 (1993) 768–771.
[2] Y. Kamio, A. Rahman, H. Nariya, T. Ozawa, K. Izaki, FEBS Lett. 321 (1993) 15–18.
[3] G. Supersac, G. Prévost, Y. Piémont, Infect. Immunol. 61 (1993) 580–587.
[4] G. Prévost, B. Cribier, P. Couppié, P. Petiau, G. Supersac, V. Finck-Barbançon, H. Monteil, Y. Piémont, Infect. Immunol. 63 (1995) 4121–4129.
[5] A.M. Woodin, The staphylococcal leukocidin, in: J.O. Cohen (Ed.), The staphylococci, Wiley, New York, 1972, pp. 281–289.
[6] B. Cribier, G. Prévost, P. Couppié, V. Finck-Barbançon, E. Grosshans, Y. Piémont, Dermatology 185 (1992) 175–180.
[7] G. Prévost, P. Couppié, P. Prévost, S. Gayet, P. Petiau, B. Cribier, H. Monteil, Y. Piémont, J. Med. Microbiol. 42 (1995) 237–245.
[8] V. Finck-Barbançon, G. Duportail, O. Meunier, D.A. Colin, Biochim. Biophys. Acta 1182 (1993) 275–282.
[9] D.A. Colin, I. Mazurier, S. Sire, V. Finck-Barbançon, Infect. Immunol. 62 (1994) 3184–3188.
[10] O. Meunier, A. Falkenrodt, H. Monteil, D.A. Colin, Cytometry 21 (1995) 241–247.
[11] T. Ozawa, J. Kaneko, Y. Kamio, Biosci. Biotech. Biochem. 59 (1995) 1181–1183.
[12] B. König, G. Prévost, Y. Piémont, W. König, J. Infect. Dis. 171 (1995) 607–613.
[13] B. König, G. Prévost, W. König, J. Med. Microbiol. (1997) in press.
[14] A.J. Siqueira, C. Speeg-Schatz, F.I.S. Freitas, J. Sahel, H. Monteil, G. Prévost, J. Med Microbiol. (1997) in press.
[15] G. Prévost, G. Supersac, D.A. Colin, P. Couppié, S. Sire, T. Hensler, P. Petiau, O. Meunier, B. Cribier, W. König, Y. Piémont, The new family of leucotoxins from *S. aureus*: structural and biological properties, in: J. Freer et al. (Eds.), Bacterial Protein Toxins, Suppl. 24, Zentralblatt für Bakteriologie, Gustav Fischer, Stuttgart, 1994, pp. 284–293.
[16] C. Yanisch-Perron, J. Viera, J. Messing, Gene 33 (1985) 103–119.
[17] R.K. Saiki, D.H. Gelfand, S. Stoffel, S. Scharf, R. Higuchi, G.T. Horn, K.B. Mullis, H.A. Erlich, Science 239 (1988) 487–491.
[18] S. Tabor, C.C. Richardson, Proc. Natl. Acad. Sci. USA 84 (1987) 4761–4771.
[19] V. Finck-Barbançon, G. Prévost, Y. Piémont, Res. Microbiol. 142 (1991) 75–85.
[20] U.K. Laemmli, Nature 227 (1970) 680–685.
[21] D. Blakeslee, J. Immunol. Methods 17 (1977) 361–364.
[22] D.W. Marquardt, J. Soc. Ind. Appl. Math. 11 (1963) 431–441.
[23] H. Byler, H. Susi, Biopolymers 25 (1986) 469–487.
[24] G. Menestrina, FEBS Lett. 232 (1988) 217–220.
[25] S. Cauci, R. Monte, M. Ropele, C. Missero, T. Not, F. Quadrifoglio, G. Menestrina, Mol. Microbiol. 9 (1993) 1143–1155.
[26] R.S. Larson, A.L. Corbi, L. Berman, T.A. Springer, J. Cell. Biol. 108 (1989) 703–712.
[27] P.Y. Chou, G.D. Fasman, Biochemistry 13 (1974) 222–245.
[28] J. Garnier, D.J. Osguthorpe, B. Robson, J. Mol. Biol. 120 (1978) 97–120.
[29] W. Choorit, J. Kaneko, K. Muramoto, Y. Kamio, FEBS Lett. 357 (1995) 260–264.
[30] G. Prévost, T. Bouakham, Y. Piémont, H. Monteil, FEBS Lett. 376 (1995) 135–140.
[31] C.J. Bailey, M.B. Redpath, Biochem. J. 284 (1992) 177–180.
[32] L. Song, M.R. Hobaugh, C. Shustak, S. Cheley, H. Bayley, J.E. Gouaux, Science 274 (1996) 1859–1866.
[33] A. Valeva, M. Palmer, K. Hilgert, M. Kehoe, S. Bhakdi, Biochim. Biophys. Acta 1326 (1995) 213–218.
[34] A. Valeva, A. Weisser, B. Walker, M. Kehoe, H. Bayley, S. Bhakdi, M. Palmer, EMBO J. 15 (1995) 1857–1864.